Adaptive Gain Processing With Offending Frequency Suppression for Digital Hearing Aids

Ashutosh Pandey and V. John Mathews, *Fellow, IEEE*

***Abstract*—Digital hearing aids identify acoustic feedback signals and cancel them continuously in a closed loop with an adaptive filter. This scheme facilitates larger hearing aid gain and improves the output sound quality of hearing aids. However, the output sound quality deteriorates as the hearing aid gain is increased. This paper presents two methods to modify the forward path gain in digital hearing aids. The first approach employs a variable, frequency-dependent gain function that is lower at frequencies of the incoming signal where the information is perceptually insignificant. The second method of this paper automatically identifies and suppresses residual acoustical feedback components at frequencies that have the potential to drive the system to instability. The suppressed frequency components are monitored and the suppression is removed when such frequencies no longer pose a threat to drive the hearing aid system into instability. Together, the gain processing methods of this paper provide 8 to 12 dB more hearing aid gain than feedback cancelers with fixed gain functions. Furthermore, experimental results obtained with real world hearing aid gain profiles indicate that the gain processing methods of this paper, individually and combined, provide less distortion in the output sound quality than classical feedback cancelers enabling the use of more comfortable style hearing aids for patients with moderate to profound hearing loss.**

***Index Terms*—Acoustic feedback, adaptive filters, gain processing, hearing aids.**

I. Introduction

A hearing aid amplifies the incoming sound to make it audible for people with hearing loss. A typical hearing loss is a sensorineural loss at higher frequencies with normal hearing at lower frequencies. Approximately 10% (30 million people) of the U.S. population suffers from some hearing loss and most of them need hearing aids. The maximum gain achievable in a hearing aid is limited by acoustic feedback, which is present mostly because of a vent that provides patients comfort from the acoustic pressure difference at the ear drum. An adaptive filter is often used to continuously estimate the feedback path and cancel the acoustic feedback in hearing aids. Fig. 1 shows the block diagram of a typical digital hearing aid with a single microphone, speaker, and adaptive feedback cancellation (AFC) implemented in the subband domain. Digital hearing aids use discrete signal samples of the microphone signal $u(n)$ and the speaker signal $x(n)$ to perform the necessary signal processing for hearing-impaired listeners. In Fig. 1, the prescribed amplification for a hearing-impaired listener is provided in the subband domain with gain values $\mathbf{g}(m)$, where the entries of the gain vector are the gain values for the subbands. The delay d_1 is used to adjust the bias in the adaptive filter estimate. The broadband variable gain function g_c can be used to adjust the overall output sound level in changing acoustic environments and is often available to hearing aid users as a volume control on the face plate of the hearing aid.

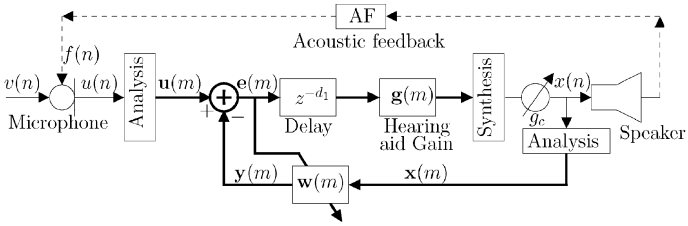

Fig. 1. Simplified block diagram of a digital hearing aid with AFC (thin and thick lines indicate scalar and vector quantities whereas m and n denote the time indices for the subband domain and fullband signals, respectively).

Adaptive feedback cancellation (AFC) improves the output sound quality and provides an additional gain over the critical gain[1] for which the hearing aid is stable [1]–[4]. When the amplification in a hearing aid is more than the limits of the maximum stable gain, the hearing aid becomes unstable or the quality of the signal degrades to below acceptable levels [2]. A major source of this loss of performance of the system is the presence of residual feedback components in the signal. If acoustical feedback components are reduced, the stability and the output sound quality of a hearing aid can be further improved. Many researchers have proposed to change the characteristics of the signal in the forward path by changing its phase, shifting its frequency components, or modifying its spectral magnitude with a notch filter to suppress the feedback and hence provide maximum stable gains [2], [5]. Although these methods keep the hearing aid stable, the output sound quality degrades as the signal characteristics are changed.

In this paper, two methods that alter the hearing aid gain in the forward path to enhance the stability of the hearing aid by reducing the acoustical coupling between the loudspeaker and the microphone. In the first method, referred as adaptive gain processing, the hearing aid gain values $\mathbf{g}(m)$ are reduced intermittently at perceptually redundant components in speech.

Manuscript received December 11, 2010; revised June 29, 2011; accepted September 21, 2011. Date of publication October 10, 2011; date of current version January 25, 2012. The associate editor coordinating the review of this manuscript and approving it for publication was Mr. James Johnston.

The authors are with the Department of Electrical and Computer Engineering, University of Utah, Salt Lake City, UT 84112 USA (e-mail: ashu503@yahoo.com).

Color versions of one or more of the figures in this paper are available online at http://ieeexplore.ieee.org.

Digital Object Identifier 10.1109/TASL.2011.2170973

[1]Critical gain refers to the maximum amplification for which the output signal quality is acceptable without feedback cancellation.

Research in psychoacoustics has shown that humans have difficulty hearing weak signals that fall in the frequency (frequency masking) or time vicinity (temporal masking) of stronger signals [6], [7]. Such components do not contribute to the understanding of speech regardless of whether they are amplified or not. Such redundancies were successfully used in the past in the area of coding and noise suppression [6], [8].

In the second method, the forward path gain is reduced at frequencies in the signal that are more likely to drive the system to unstable behavior. We refer to the frequencies so identified as the *offending frequencies* (OF). If offending frequencies are detected accurately and gain is reduced in a narrowband frequency region around these frequencies, the gain reduction is not audible for a few offending frequencies [9], [10]. This approach is similar to methods for controlling acoustical feedback in public address (PA) systems using narrowband parametric equalization (EQ) filters [11]. We call this method offending frequency suppression in this paper.

Specifically, the offending frequencies are detected as they begin to develop instabilities in the system. The gain is reduced with narrowband parametric equalization (EQ) filters. While offending frequency suppression results in more stable hearing aids, the changes in offending frequencies are not tracked in traditional methods. This can result in unwanted gain reductions at several frequencies in the signal over long periods of time. Traditionally, in public address (PA) systems, parametric EQ filters are reset (removed from the forward path) periodically and new offending frequencies are detected upon reset. However, this is not the most desired method because until the offending frequencies are reset, there may be unnecessary distortion in the system. In this paper we develop a method that monitors the adaptive feedback canceller coefficients to reset the parametric EQ filters when the offending frequencies change. The offending frequency suppression and reset method provide substantial amount of maximum stable gain with minimal impact on the perceptual quality of the output signal.

The two ways of reducing hearing aid gain have been partially presented by the authors in two conference papers [12], [13]. In this paper, we develop control algorithms to combine both methods with the offending frequency reset algorithm, present a modified offending frequency suppression method more suitable for hearing aids and music signals and, exhaustively evaluate the hearing aid gain system with real world hearing aid gain profiles, feedback path models and speech/music signals.

The rest of the paper is organized as follows. Section II provides a description of a classical transform domain hearing aid system. The hearing aid gain processing methods—adaptive gain processing and offending frequency suppression with the reset algorithm to remove offending frequency suppression filters are presented and discussed in Section III. In Section IV, the performance of both gain processing algorithms is evaluated and compared, separately and jointly, in MATLAB as well as from real-time implementations. We make the concluding remarks in Section V.

II. Fixed Gain Transform Domain Signal Processing

For performance comparisons, we will use a subband-based system employing M subbands, which are created with over-sampled generalized discrete Fourier transform (GDFT) filter banks [14]–[17]. Each subband component operates at $L \leq M$ times lower sampling rate than the full sampling rate of the system. The GDFT filter banks are known for their computationally efficient implementation via fast Fourier transform (FFT) [18]–[20]. Let $u_i(m)$ and $x_i(m)$ denote subband domain signals in band i at time m for the microphone and speaker, respectively. Other signals follow a similar notation in the subband domain for this paper. Gain compensation for hearing loss and adaptive feedback cancellation are done in the subband domain. Gain compensation is done by adjusting the subband gain values $g_i(m)$ based on a frequency dependent audiogram of the hearing-impaired listener. We call this a fixed gain system because the gain values do not change with time.

TABLE I
Update Equations for a Subband-Based AFC

$$\mathbf{x}_i(m) = \begin{bmatrix} x_i(m) & x_i(m-1) & \cdots & x_i(m-N_s+1) \end{bmatrix}^T$$
$$\mathbf{w}_i(m) = \begin{bmatrix} w_i^0(m) & w_i^1(m) & \cdots & w_i^{N_s-1}(m) \end{bmatrix}^T$$
$$e_i(m) = u_i(m) - y_i(m) = u_i(m) - \mathbf{w}_i^T(m)\mathbf{x}_i(m)$$
$$\mu_i(m) = \frac{\alpha}{\|\mathbf{x}_i(m)\|^2 + \zeta}$$
$$\mathbf{w}_i(m+1) = \mathbf{w}_i(m) + \mu_i(m)e_i(m)\mathbf{x}_i(m)$$

Finally, adaptive feedback cancellation is done with a normalized adaptive least-mean-square algorithm (NLMS) algorithm in each subband. Subband adaptive filters together model a full band feedback path that is approximated with a linear impulse response with N coefficients. Let $\mathbf{w}_i(m)$ represent the adaptive filter coefficient vector for the ith subband and contain $N_s = [N/L]$ coefficients, where the operation $[a]$ returns the integer part of the real number a. If N is not a multiple of L, modeling the adaptive filter with N_s coefficients in subband is not an exact but close approximation of the impulse response with N coefficients in full band. The update equations for the NLMS adaptation in the ith subband for the mth subband sample to estimate the feedback path are given in Table I. In Table I, α is a small positive constant that controls the adaptation speed of the system and ζ is another small positive constant designed to avoid a divide-by-zero [21].

III. Hearing Aid Gain Processing Methods

In the traditional system described in Section II, the hearing aid gain in the forward path consists of a prescribed hearing aid gain that is time-invariant and independent of the input signal and a time-varying nonlinear gain processing algorithms to perform noise reduction (NR) and wide dynamic range compression (WDRC). The methods of this paper alter the prescribed hearing aid gain in the forward path with the hearing aid gain values and parametric EQ filters in addition to this type of processing. For simplicity and to exclusively evaluate benefits of the methods of this paper, we assume that the hearing aid provides fixed gain to the hearing aid user. Interaction of the methods of this paper with WDRC and NR is provided towards the end of this paper. A block diagram of the new scheme employing the gain processing methods of this paper is shown in Fig. 2. First, the system applies adaptive

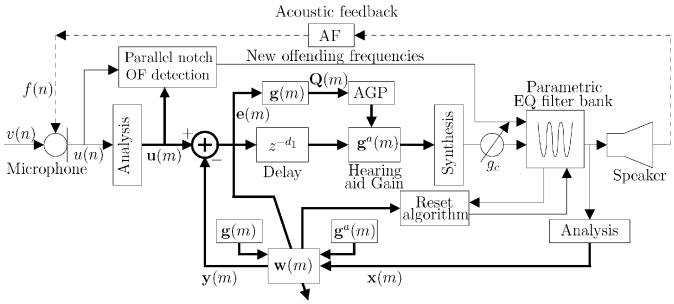

Fig. 2. Simplified block diagram of a digital hearing aid employing AGP and OFS along with AFC.

gain processing (AGP) by calculating the masking thresholds from the target amplified signal $\mathbf{Q}(m)$, and uses that to modify the gain values in the each subband. The modified gain values are referred as $\mathbf{g}^a(m)$. The modified gain values $\mathbf{g}^a(m)$ and prescribed gain values $\mathbf{g}(m)$ are also used to modify step size for NLMS adaptation. The details of modifying gain values $\mathbf{g}^a(m)$ and step size control are presented in Section III-A.

Second, the new scheme identifies potential offending frequencies from the microphone signal. The forward path gain is reduced in narrowband frequency bands at those frequencies using parametric EQ filters as shown in Fig. 2. The change in offending frequencies is monitored with a reset algorithm that uses subband adaptive filter coefficients $w_i(m)$. The offending frequency suppression (OFS) and the reset methods are described in Section III-B.

A. Adaptive Gain Processing

The adaptive gain processing (AGP) utilizes the information about masking thresholds in the target amplified signal. We describe the steps involved in finding the masking thresholds in Section III-A1. Gain and step size control schemes that result in low artifacts and low distortions in the output signals are discussed later in the section.

1) Calculation of Masking Thresholds: Masked signal components are considered as "irrelevant information" and it is shown in literature that even well trained human ears do not hear these components. In this paper, we do not consider the contribution of temporal masking because frequency domain masking has the stronger effect [7]. Spectrally masked components used in this paper are identified with psychoacoustic principles such as absolute hearing thresholds, critical band frequency analysis, and the spreading function. Calculation of the masking thresholds $T_i(m)$ for the mth frame and ith subband involves defining critical bands on the power spectrum $P_i(m)$ of the speech signal. The power spectrum is calculated from the spectrum of the target amplified signal $Q_i(m)$ using speech pressure level (SPL) normalization [6]. Subsequently, tonal and noise maskers are identified in each critical band which are above the hearing threshold [6], [7], [22]. If two or more maskers are close to each other in a critical band, only the strongest masker is kept and others are discarded. Details of the masking model and estimation of the maskers can be found in [6], [8]. After identifying the maskers, the masking effects due to these maskers are calculated using a spreading function [22]. Finally, the global masking threshold $T_i(m)$ is calculated for each subband by combining the individual masking thresholds of all the maskers identified in the previous steps.

TABLE II
ADAPTIVE GAIN PROCESSING

Initialization

$g_i^a(0) = g_i(0)$ ... for each subband i

Gain update

$$p_i^r(m) = \begin{cases} 0 & \text{if } |Q_i(m)|^2 < T_i(m) \\ 1 & \text{else} \end{cases}$$

$$g_i^a(m) = p_i^r(m) g_i(m) + (1 - p_i^r(m)) \eta g_i^a(m-1)$$

$$g_i^a(m) = \max[g_i^a(m), \eta_m g_i(m)]$$

2) Gain Adjustment With $T_i(m)$: The adaptive gain processing algorithm reduces the hearing aid gain at subbands where the instantaneous signal energy ($|Q_i(m)|^2$) is below the global masking threshold $T_i(m)$. However, a large reduction in the gain may produce artifacts due to aliasing [1]. Consequently, the algorithm reduces the gain by no more than some preselected fraction η, where $0 < \eta < 1$ from frame to frame. Similarly, we also limit the minimum gain at a frequency to avoid unnatural artifacts in the output. The adaptive gain processing maintains the gain to prescribed levels as soon as the signal strength is above the masking threshold. It must be mentioned that, the AGP increases the hearing aid gain to prescribed levels as soon as the signal strength is above the masking threshold in the current frame irrespective of the gain value in the previous frame. We have not experienced any artifacts due to sudden changes, however, a gradual increase in gain similar to what employed for reducing the hearing aid gain can be used if needed.

The algorithm for varying the gain $g_i^a(m)$ is summarized in Table II where $\eta_m < 1$ is a positive constant that determines the minimum permissible gain based on the prescribed gain value $g_i(m)$ for the ith subband.

3) Step Size Control for Adaptive Gain Processing: It is intuitive to see that the better the adaptive filter estimates the feedback path, the more stable is the hearing aid system. Interestingly, for fixed step size α, the error between the adaptive filter estimate and the true feedback path in a hearing aid system shown in Fig. 1 depends on the hearing aid gain [1], [3]. Let us define the coefficient error vector in the adaptive filter estimate for band i at time m as

$$\widetilde{\mathbf{w}}_i(m) = \mathbf{h}_i - \mathbf{w}_i(m) \tag{1}$$

where $\mathbf{h}_i = [h_i^0 \; h_i^1 \; \cdots \; h_i^{N_s-1}]^T$ represents true feedback path coefficient vector for band i. For the derivations, we assume the feedback path is time-invariant. The steady state misalignment $E[|\tilde{w}_i|^2]$ is approximated by $\alpha/2g_i^2(m)$ as shown in [3]. In fixed gain systems, the gain values $g_i(m)$ is constant over time. Consequently, the steady state misalignment does not change. However, the adaptive gain processing varies the subband gain values $g_i^a(m)$ depending on the input signal. If the hearing aid gain is reduced in a band, the error in the adaptive filter estimate (misalignment) will increase. Subsequently, if the gain is increased suddenly in that band, the adaptive filter will take sometime to adapt to the new (better) estimate. In order to avoid

TABLE III
UPDATE EQUATIONS FOR A SUBBAND-BASED AFC SYSTEM EMPLOYING THE ADAPTIVE GAIN PROCESSING

$$\alpha_i^a(m) = \alpha \left(\frac{g_i^a(m)}{g_i(m)} \right)^2$$
$$\mu_i^a(m) = \frac{\alpha_i^a}{\|\mathbf{x}_i(m)\|^2 + \zeta}$$
$$\mathbf{w}_i(m+1) = \mathbf{w}_i(m) + \mu_i^a(m) e_i(m) \mathbf{x}_i(m)$$

TABLE IV
CALCULATION OF THE COEFFICIENTS OF THE EQ FILTERS

$$K = \tan(\frac{2\pi f_p}{f_s}),\ \beta = 1 + K/q + K^2$$
$$b_0 = \frac{1 + pK/q + K^2}{\beta},\ b_1 = \frac{2(K^2 - 1)}{\beta},\ b_2 = \frac{1 - pK/q + K^2}{\beta}$$
$$a_0 = 1.0,\ a_1 = \frac{2(K^2 - 1)}{\beta},\ a_2 = \frac{1 - K/q + K^2}{\beta_i}$$

the readaptation of adaptive filter, we vary the adaptation parameter to keep the misalignment independent of the hearing aid gain change due to the adaptive gain processing. The variable adaptation parameter $\alpha_i^a(m)$ is based on the current hearing aid gain value $g_i^a(m)$ and prescribed hearing aid gain value $g_i(m)$. This scheme will avoid additional error in the adaptive filter coefficients when hearing aid gain is reduced for a short period of time. Based on the above two gain values, the adaptation parameter $\alpha_i^a(m)$ and the NLMS update for band i at time m for the adaptive gain processing is done as shown in Table III.

Traditional hearing aid systems employing adaptive gain processing such as WDRC and NR can employ a similar step-size control to keep the misalignment independent of the hearing aid gain processing.

B. *Offending Frequency Suppression*

The offending frequency suppression method presented in this paper identifies offending frequencies that are likely to drive the hearing aid system into instability and uses parametric EQ filters [11] to reduce gain at those frequencies.

The acoustic feedback components are known to grow steadily in successive time intervals whereas the audio components behave otherwise in many cases. Therefore, if energy in a subband is increasing in successive time intervals, it is likely that there exist an offending frequency within the frequency range of that subband. Monitoring just the energy can falsely detect some MUSIC signals as acoustic feedback since many components of music can exhibit similar characteristics to the feedback components. We used multiple characteristics and the history of such behaviors to reduce false alarms. The more the history or characteristics are used, the smaller are the false alarms. However, this will delay the detection of the acoustic feedback. In this paper, we have used energy growth and the behavior the adaptive filters to identify the acoustic feedback. Specifically, the offending frequency within that subband is accurately estimated with an adaptive notch filter whose center frequency is constrained to the frequency range of the subband. Adaptive notch filters can identify offending frequencies because they behave like tonal signals [9], [23]. At high gains, as the hearing aid system nears unstable behavior, the energy in the signal components at and around the offending frequencies increases in the forward path of the hearing aid and creates spectral peaks. The adaptive notch filter (ANF) tracks and identifies such spectral peaks. In the presence of such spectral peaks, the ANFs will converge to the offending frequencies and stay in their vicinities till the energy in such spectral components reduces. The variability of the coefficients of the ANF will be small when the system is tracking a strong frequency component than when the input signal does not contain strong spectral peaks. Consequently, our approach uses the variability of the notch frequency of the ANF as the other measure for accurately detecting the offending frequencies.

The adaptive notch filters can also be implemented in the subband domain without loss of performance. However, we chose to implement the ANFs in the fullband. M adaptive notch filters are used to monitor frequency ranges for M subbands. Similarly, M energy growth monitoring values, one from each subband, are used for detection of an offending frequency. The detection method immediately starts to look for another offending frequency after detection of an offending frequency in a subband. More details are provided in Section III-B1.

Upon detection of an offending frequency, a parametric EQ filter is used to suppress it. The parametric EQ filter employed in this work is a second-order infinite impulse response (IIR) filter that is specified by three parameters—the center frequency f_p, the depth of suppression $p < 1$ and quality factor q [24]. The parameters p and q are fixed in our implementation whereas the parameter f_p is derived from the adaptive notch filter. Coefficients of the parametric EQ filter in the discrete-time domain with the transfer function

$$H_{EQ}(z) = \frac{b_0 + b_1 z^{-1} + b_2 z^{-2}}{a_0 + a_1 z^{-1} + a_2 z^{-2}} \tag{2}$$

can be calculated from the parameters p, q and f_p as given in Table IV. The variable f_s in Table IV represents the sampling frequency.

1) Detection of Offending Frequencies With ANFs and Energy Growth Monitoring in Subbands: As stated earlier, the offending frequencies are detected independently for each subband. In this section, we explain offending frequency detection in the ideal frequency range of the ith subband—$[f_i^l, f_u^l]$, where $f_i^l = 2\pi i/M$ is the lower frequency and $f_i^u = 2\pi(i+1)/M$ is the upper frequency of the band $i, = 0 \cdots M-1$. By monitoring frequency ranges associated with all subbands, we can detect any offending frequency occurring in the operating frequency range of the hearing aid.

The energy growth monitoring and ANF tracking for the ith frequency range (f_i^l to f_i^u) work independently in the subband and fullband, respectively. The energy growth monitoring is performed for each subband microphone signal $u_i(m)$ whereas the adaptive notch filter works with the fullband microphone signal $u(n)$. Let the microphone signal energy in band i at time m be $P_i^u(m) = \mathbf{u}^T(m)\mathbf{u}(m)$, where $\mathbf{u}_i(m) = [u_i(m)\ u_i(m -$

$1) \cdots u_i(m-N_s+1)]^T$. The relative change in the microphone energy between two successive time intervals $P_i^{\Delta}(m)$ defined as

$$P_i^{\Delta}(m) = \frac{P_i^u(m) - P_i^u(m-1)}{P_i^u(m-1)}$$

along with the estimated microphone signal energy $P_i^u(m)$ and the estimated background noise signal power $P_i^b(m)$ are used by the counter $\gamma_i^r(m)$ to monitor the energy growth for the ith subband at time m. Larger values of the counter $\gamma_i^r(m)$ makes the band i more probable to contain an offending frequency.

The counter is incremented if the microphone signal $P_i^u(m)$ is at least T_b times larger than the background noise power[2] $P_i^b(m)$ for band i. Otherwise, it is reset to 0 to indicate that the system is stable. If the energy in the microphone signal is higher than the predetermined multiple of the background noise power and the energy in the microphone signal at time m is greater than the energy at time $m-1$, i.e., the relative change in the energy $P_i^{\Delta}(m)$ is positive, the energy growth counter value is incremented by $\Gamma_u > 0$. On the other hand, the energy growth counter $\gamma_i^r(m)$ is reduced by an amount $\Gamma_l < 0$, if the relative change is smaller than a predetermined negative constant ν_l. This is because sudden decrease in the energy is not a characteristics of the acoustic feedback components at the onset of instability. Additionally, if the relative change in energy $P_i^{\Delta}(m)$ is negative, however the change is small, say $\nu_u < 0$, the energy growth counter is still increased by Γ_u. This is because a small change in energy may indicate early stages of howling [13]. In other situations, where the relative change in energy $P_i^{\Delta}(m)$ lies between ν_l and ν_u, the energy growth counter is modified with a number that is linear interpolation between Γ_l and Γ_u. The amount of change in the energy growth counter at time m for a given $P_i^{\Delta}(m)$ is defined by a function $\Phi(P_i^{\Delta}(m))$ as

$$\Phi\left(P_i^{\Delta}(m)\right) = \begin{cases} \Gamma_u, & P_i^{\Delta}(m) > \nu_u \\ \Gamma_l, & P_i^{\Delta}(m) < \nu_l \\ \frac{\Gamma_u - \Gamma_l}{\nu_u - \nu_l}\left(P_i^{\Delta}(m) - \nu_l\right) + \Gamma_l, & \text{otherwise.} \end{cases}$$

The complete energy growth calculation is described in Table V. It is easy to see from Table V that if the microphone signal $P_i^u(m)$ is sufficiently above (T_b times) the noise floor $P_i^b(m)$ and the relative change in energy is positive or close to zero in successive time indexes, the energy growth counter $\gamma_i^r(m)$ grows. On the other hand, if it is relatively negative ($< \nu_u$), the energy growth counter will tend to a minimum value γ_m^r. If the energy growth counter $\gamma_i^r(m)$ exceeds a predetermined threshold T_r, one of the two criteria for band i to have an offending frequency is fulfilled. The other criterion is determined using adaptive notch filters as described next.

The microphone signal $u(n)$ in Fig. 1 is used as the input signal to the adaptive notch filter for calculating the center frequency for each parametric EQ filter employed to suppress an offending frequency. In addition, the adaptive notch filters are also used to detect onset of instability along with the energy growth counters. We employ a second-order notch filter with input–output relationship of the form

$$H_a(z) = \frac{1 - a(n)z^{-1} + z^{-2}}{1 - \rho a(n)z^{-1} + \rho^2 z^{-2}} \tag{3}$$

to suppress the offending frequencies for band i. The ANF adjusts to the center frequency of the notch filter by adjusting parameter $a_i(n)$ such that at time n the output power of the notch filter $z_i(n)$ is reduced [9]. The parameter $a_i(n)$ is constrained to adapt between $[2\cos(2\pi f_i^u), 2\cos(2\pi f_i^l)]$ to track the frequency range of the ith subband—$[f_i^l, f_i^u]$. The update equations for the adaptive notch filter realized in direct-form II are summarized in Table V. In Table V, λ_s is a suitable averaging constant, α_a is the step size for adaptation and ϵ_a is a small positive constant to prevent singularities.

The second parameter we employ to detect onset of instability is the variability of the coefficients of the notch filter. It has been observed [13] that the adaptive filters coefficients show little variability in the presence of the strong tonal signals. The variability of the parameter $a_i(n)$ from the mean of its past values $a_i^m(n)$ is monitored with a counter $\gamma_i^a(n)$. The mean $a_i^m(n)$ is estimated by averaging past values of $a_i(n)$ with a single pole IIR filter with an averaging constant λ_m. If the parameter $a_i(n)$ does not vary significantly from its mean as determined by a preselected threshold δ_q, the counter $\gamma_i^a(n)$ grows; otherwise it is reset to 0. If the counter $\gamma_i^a(n)$ gets larger than a predetermined threshold T_a, and the energy growth counter $\gamma_i^r(m)$ becomes larger than a predetermined threshold T_r, the system determines

TABLE V
OFFENDING FREQUENCY DETECTION IN THE ith BAND

Adaptive notch filter update

$$s_i(n) = u(n) + \rho a_i(n-1)s_i(n-1) - \rho^2 s_i(n-2)$$
$$z_i(n) = s_i(n) - a_i(n-1)s_i(n-1) + s_i(n-2)$$
$$P_i(n) = \lambda_s P_i(n-1) + (1-\lambda_s)s_i^2(n-1)$$
$$a_i(n) = a_i(n-1) + \frac{\alpha_a}{P_i(n)+\epsilon_a} s_i(n-1)z_i(n)$$
$$a_i(n) = \begin{cases} 2\cos(2\pi f_i^l) & ; a_i(n) > 2\cos(2\pi f_i^l) \\ 2\cos(2\pi f_i^u) & ; a_i(n) < 2\cos(2\pi f_i^u) \\ a_i(n) & \text{;otherwise} \end{cases}$$

ANF tracking monitor

$$a_i^m(n) = \lambda_m a_i^m(n-1) + (1-\lambda_m)a_i(n)$$
$$\gamma_i^a(n) = \begin{cases} \gamma_i^a(n-1) + 1 & ; |a_i(n) - a_i^m(n)| < \delta_q \\ 0 & \text{;otherwise} \end{cases}$$

Energy growth monitor

$$P_i^u(m) = \mathbf{u}^T(m)\mathbf{u}(m)$$
$$\overline{P_i^u(m)} = \lambda_u \overline{P_i^u(m-1)} + (1-\lambda_u)P_i^u(m)$$
$$P_i^b(m) = \min(\delta_b P_i^b(m-1), \overline{P_i^u(m)})$$
$$\gamma_i^r(m) = \begin{cases} \gamma_i^r(m-1) + \Phi(P_i^{\Delta}(m)) & ; P_i^u(m) > T_b P_i^b(m) \\ 0 & \text{;otherwise} \end{cases}$$
$$\gamma_i^r(m) = \max(\gamma_i^r(m), \gamma_m^r)$$

Offending frequency detection (when $n = Lm$)

if $\gamma_i^a(n) > T_a$ and $\gamma_i^r(m) > T_r$
$\Rightarrow$ Offending frequency detected
$\Rightarrow$ Add a parametric EQ at $\frac{1}{2\pi}\cos^{-1}(a(n)/2)$
$\Rightarrow \gamma_i^a(n) = 0, \gamma_i^r(m) = \gamma_m^r$

[2]In this paper, the background noise is estimated with the minimum statistics method according to [25]. In Table V, the constant $\delta_b > 1$ is the slow rising constant, λ_u is an averaging constant and $\overline{P_i^u(m)}$ is the average microphone signal for band i at time m. These quantities are required in the minimum statistics method.

that the hearing aid may go unstable (howl) at or around the notch frequency. When both thresholds are exceeded, a parametric EQ filter whose center frequency is derived from the current value of $a_i^m(n)$ as $(1/2\pi)\cos^{-1}(a_i^m(n)/2)$ is applied to the output signal and the counters $\gamma_i^a(n), \gamma_i^r(m)$ are reset to 0.

2) Resetting Offending Frequency Suppression Filters: Offending frequencies are identified at the onset of instability near that frequency. The offending frequency suppression method of this paper places parametric EQ filters to suppress offending frequencies when they are detected. In practice, new offending frequencies appear because the acoustic feedback path of the hearing aid and the signal characteristics change [26]. The feedback path of the hearing aid changes if a person moves closer to a reflective surface, brings a telephone receiver close the face plate of a hearing aid, wears a hat, etc. While new offending frequencies will appear inevitably during the operation of a hearing aid, it is possible that some of the old offending frequencies are no longer problematic. In other words, if parametric EQ filters at those old frequencies are removed from the loop, the system will not go into instability.

Traditionally, commercial offending frequency suppression methods in PA systems employ periodic reset of offending frequencies to remove unnecessary parametric EQ filters. In this paper, we use analysis of the adaptive filter coefficients to reset offending frequencies by removing the parametric EQ filters. Furthermore, we monitor each subband independently to track the changes in different frequency regions. The reset method calculates relative change in the current adaptive filter estimate from its older estimates. If the relative change between the current and old estimates is small, we assume no change in the feedback path. Therefore, offending frequencies are not modified. On the other hand, if the change is larger than a predetermined threshold, the offending frequencies are reset—parametric EQ filters are removed.

Specifically, the reset algorithm uses two measurements of the adaptive filter coefficients $\mathbf{w}_i(m)$. First, a long term average $\mathbf{L}_i(m)$ of the adaptive filter coefficients for the ith band at time m is estimated using a single pole IIR filter with averaging constant $\lambda_l, 0 < \lambda_l < 1$. This is treated as a measure of the past stable path of the feedback path at time m. A short term average $\mathbf{M}_i(m)$ of the adaptive filter coefficients for the ith band at time m is also estimated with an averaging constant λ_h where the averaging constant is such that $0 < \lambda_h < \lambda_l < 1$. The short term average is treated as a measure of the current state of the feedback path. If the distance between the short term average differs significantly from the long term average for a few iterations, say T_o, the system assumes that the feedback path has changed for that band. In this event, any parametric EQ filters that fall in the frequency range of that band are removed. The reset algorithm for the ith band at time m is listed in Table VI. In Table VI, $\mathbf{D}_i(m)$ is the distance vector and $\kappa_i(m)$ is the normalized distance between the long term and short term average measurements. The normalized distance $\kappa_i(m)$ remains close to 0 if the feedback path is relatively stationary and increases in magnitude when there are changes in the feedback path. The variable $\gamma_i^o(m)$ counts the number of times the normalized distance has been more than a predetermined threshold δ_o to trigger reset process.

TABLE VI
EQUATIONS FOR THE RESET ALGORITHM IN THE ith BAND

Initialization

$\mathbf{L}_i(0)$ ... A column vector of length N_s with all zeros
$\mathbf{M}_i(0)$ ... A column vector of length N_s with all zeros
$\gamma_i^o(0)$ ... 0

Reset algorithm

$$\mathbf{L}_i(m) = \lambda_l \mathbf{L}_i(m-1) + (1-\lambda_l)\mathbf{w}_i(m)$$
$$\mathbf{M}_i(m) = \lambda_h \mathbf{M}_i(m-1) + (1-\lambda_h)\mathbf{w}_i(m)$$
$$\mathbf{D}_i(m) = \mathbf{L}_i(m) - \mathbf{M}_i(m)$$
$$\kappa_i(m) = \frac{\mathbf{D}_i^T(m)\mathbf{D}_i(m)}{\mathbf{L}_i^T(m))\mathbf{L}_i(m) + \epsilon_r}$$
$$\gamma_i^o(m) = \begin{cases} \gamma_i^o(m-1)+1 & ;\kappa_i(m) > \delta_o \\ 0 & ;\text{otherwise} \end{cases}$$

Detection

if $\gamma_i^o(n) > T_o$

$\Rightarrow$ Remove all parametric EQs between frequencies f_i^l and f_i^u

IV. RESULTS AND DISCUSSION

This section presents the results from MATLAB simulations and real time implementations of the hearing aid algorithms to demonstrate the performance of the paper's gain processing approaches. In order to evaluate the benefits due to the gain processing methods presented in this paper, we compare these methods against the hearing aid system in Section II with fixed prescribed hearing gain and no nonstationary hearing aid gain processing. Both methods were evaluated in terms of output sound quality and maximum stable gain. The true feedback path was simulated using a 192-tap FIR filter in parallel with a homogeneous quadratic nonlinearity. The nonlinearity simulates the nonlinear distortions in the loudspeakers and A/D converters in a hearing aid system as reported in literature [27], [28]. The harmonic signal strength was 40 dB below that of the output of the linear component that was selected from the range of distortions reported in the literature.

Coefficients for the linear component of the feedback paths were obtained from measurements of an inside-the-ear (ITE) hearing aid. The ITE hearing aid consisted of two FG-3653 omnidirectional microphones and a receiver. The output of the microphones and input to the receiver were available at the face plate of the hearing aid as CS44 plugs. We used a standard EXPRESSfit hearing aid programming cable to drive and access microphones and the speaker of the hearing aid. The programming cable was connected to an interface board through an 8-pin mini DIN plug that provided the required power to the programming cable and amplified the signals. Two feedback paths were used in the experiments. In estimating the feedback paths, the ITE hearing aid was fitted into the earpiece of a Knowles Electronic Manikin for Acoustic Research (KEMAR) that was placed in a quiet location. A large white board on a stand was placed parallel to the face plate of the ITE hearing aid at different distances to create different feedback paths. The white board worked as a reflective surface and was chosen to see the effect of reflective surfaces on the hearing aid feedback paths. The reflective surface was 100 cm and 5 cm away for the first

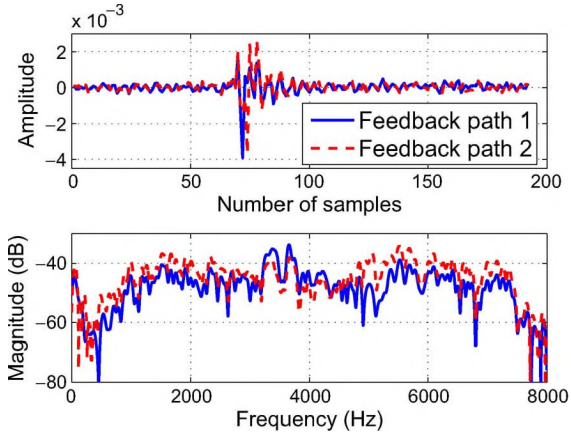

Fig. 3. Impulse and magnitude responses of the two feedback path models used in the simulations.

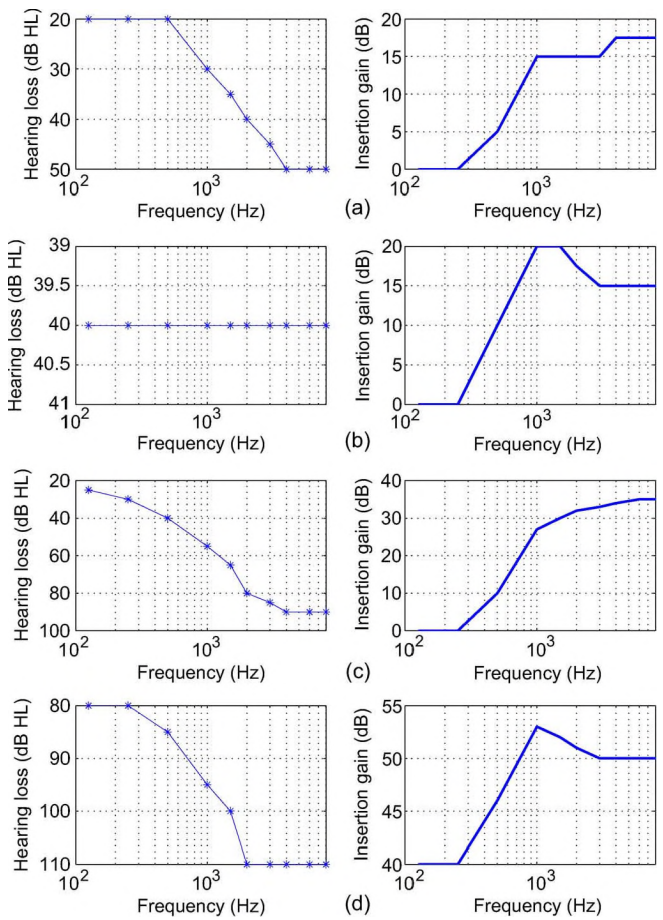

Fig. 4. Hearing loss profile and insertion gain of (a) mild-gently sloping hearing loss, (b) moderately-flat hearing loss, (c) moderate-steeply sloping hearing loss, and (d) profound-gently sloping hearing loss.

and second feedback path, respectively. Impulse and magnitude responses of the two feedback paths are shown in Fig. 3.

The feedback canceller employed a linear FIR system model with 128 coefficients. This undermodeling and the model mismatch attempt to capture the practical situation where it is very difficult to exactly model the feedback path in the system. Our prior work has indicated similar levels of performance during simulation and real-time implementations of other hearing aids. The signal processing was done at a sampling rate of $f_s = 16\,000$ Hz. Parameters of the subband design were $M = 128$, $L = 16$, $L_p = 128$. Parameters for the AFC were $\alpha = 0.001$, $d_1 = 0$, $g_c = 1$, and $\zeta = 10^{-7}$. Parameters for the hearing aid gain processing were $\eta = 0.95$ and $\eta_m = 0.1$. The overall processing delay of the system was 8 ms.

The speech input signals to the hearing aid were six clean speech waveforms of length 80 seconds taken from the TIMIT database. The peak value of the speech input signals used in experiments was approximately -6 dBu. In experiments where music signals were used, six music waveforms of length 80 seconds from the album "18 till I die" by Bryan Adams were chosen. The music signals were resampled at 16 000 Hz for the experiments. The gain of each music file was adjusted so that the peak value is no more than -6 dBu. Colored noise samples, with the power spectral density reducing at the rate of 3 dB per octave as the frequency increases, were added to simulate a noisy signal with 40-dB signal-to-noise ratio. This noise model was chosen to represent the hardware noise due to circuits/sensors in the hearing aid. The maximum hearing aid gain value used in the experiments was 61 dB. The output was clipped if the output signal became greater than 80 dBu.

To assess performance of the fixed gain system and the method of this paper, four hearing aid profiles—mild-gently sloping loss,[3] moderate-flat loss, moderate-steeply sloping loss, and profound-gently sloping loss—as shown in Fig. 4(a)–4(d) were used. The hearing loss thresholds across various frequency ranges are determined at the time of hearing aid fitting with the pure tone audiogram, commonly at frequencies 125, 250, 500, 1000, 1500, 2000, 3000, 4000, 6000, and 8000 Hz [3]. A digital hearing aid attempts to provide the insertion gain for a hearing aid patient for a given hearing loss profile. The shape of the insertion gain does not necessarily follow the shape of the hearing aid loss profile and depends on the prescription method. The insertion gains for the hearing loss profiles used in this paper were obtained with the NAL-RP prescription [30] and are shown in Fig. 4(a)–4(d). In addition, we also used many flat[4] insertion gain values to find maximum stable gains for all methods.

Unless stated otherwise, the initial value of hearing aid gain was set to 20 dB below the target gain. Subsequently, the gain was slowly increased for 20 seconds at the rate of 1 dB/s to reach the target gain level. The slow ramping up of the gain is sometimes used in commercial hearing aids when the hearing aid is programming to provide the necessary amplification for the first time. Suddenly applying the gain may cause unwanted howling in the hearing aid because the adaptive filter is starting from a reset position. Kaelin *et al.* [1] applied ramping up of the gain at the detection of feedback path change to avoid howling. The adaptive feedback cancellation experiment ran for 80 seconds in each case. The last 10 seconds of the experiment were deemed as the steady state. Psychoacoustic measures were obtained from the steady state signals to judge the performances of various schemes. In some cases, we also employed the perceptual evaluation of speech quality (PESQ) measure [31] to obtain

[3]In the definition of a hearing loss profile, the first word suggests the degree of hearing loss and the second hyphenated word suggests the hearing loss shape across frequency [29].

[4]Same gain at all frequencies.

TABLE VII
DESCRIPTION OF RATINGS TO THE SUBJECT

Ratings	Feedback	Loudness
0	Loud howling	Inaudible
1	Loud continuous whisting	Soft
2	Soft continuous whistling	Somewhat soft
3	Soft intermittent whistling	Comfortable
4	No audible feedback, acceptable quality	Somewhat loud
5	No audible feedback, good quality	Extremely loud

an easy-to-compute quantitative measure of perceptual quality of the signals. PESQ is an objective measure that analyzes a test speech signal after temporal alignment with corresponding reference signal based on psychoacoustic principles. PESQ provides perceptual quality rating of a speech segment between -0.5 and 4.5 and can be interpreted as follows. The highest score indicates that the speech signal contains no audible distortions and it is virtually identical to the clean speech segment. The PESQ scores between -0.5 and 1 indicate that the distortions and residual noise in the speech signal are very high and the segment sound unacceptably annoying. The ratings of 4, 3, 2 can be interpreted as "good quality," "slightly annoying," and "annoying," respectively. We also performed an informal subjective evaluation of the steady state data. The subjects evaluated the feedback canceled audio for the amount of residual feedback components and loudness perception. To assess the feedback components, the subjects were asked to characterize the amount of feedback components (whistling, ringing, howling) perceived in each sentence into one of the six classes enumerated in Table VII.

Loudness ratings refer to the volume of the words in each sentence. The subjects were asked to rate the loudness on a scale of 0–5. 0 indicates that the sentence is inaudible, a 5 means that the sentence is uncomfortably loud, and a 3 is the most comfortable level of sound. To obtain psychoacoustic measures, six normal-hearing listeners participated in the listening test. In order to work with normal-hearing listeners, the output of the hearing aid system was further processed with long linear-phase filters that equalized for the effects of the insertion gain of the hearing aid. The processed sounds were presented to subjects in both ears with a pair of headphones in a quiet place. Before the subjects started the experiment, they were provided with an example of the clean sound as well as example sounds of various types of artifacts for listening. The subjects always had access to the clean audio while rating the processed sounds. Since the processed signals normalized for the insertion gain, the clean reference signal had the same frequency response as the processed signals. The processed signals for the different simulated losses were presented in a random order to the user for subjective ratings.

The global masking thresholds $\mathbf{T}(m)$ for different subbands for one signal frame from a MATLAB simulation are shown in Fig. 5. In Fig. 5, the masked thresholds were calculated for normal hearing. The feedback path model 1 was used in this experiment. The hearing aid gain was flat 5 dB above the critical gain. It can be seen from Fig. 5 that there were many frequency components below the masking threshold in this simulation. This indicates that the algorithm is able to reduce the gain

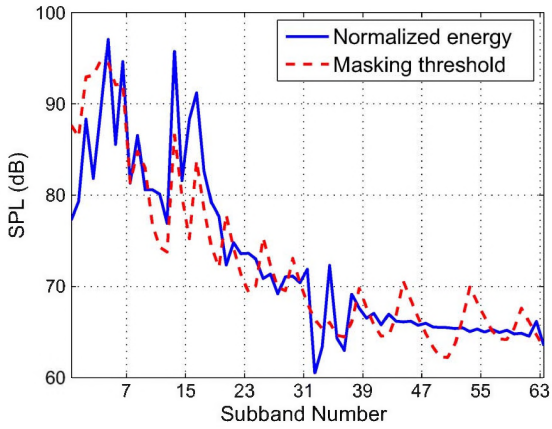

Fig. 5. Masking thresholds at various subbands.

for a large number of input signal components without reducing the perceptual quality of the output of the hearing aid.

In the first experiment, we demonstrate the ability of the system to detect and suppress offending frequencies. We disabled the adaptive feedback canceller to evaluate the behavior of the offending frequency detection algorithm. Feedback path 1 was used for this experiment and the hearing aid gain was set flat at 36.1 dB which is 0.5 dB above the critical gain for the feedback path. The parameters for detection of offending frequencies with adaptive notch filters and energy growth monitoring were $\rho = 0.95$, $\alpha_a = 0.005$, $\lambda_s = 0.99$, $\epsilon_a = 10^{-5}$, $\lambda_m = 0.99$, $\delta_q = 0.05$, $T_a = 750$, $\nu_u = -0.01$, $\nu_l = -0.1$, $\Gamma_u = 1$, $\Gamma_l = -4$, $\gamma_m^r = -20$, $T_r = 75$, $\delta_b = 1.0003$, $\lambda_u = 0.99$, and $T_b = 6$. Parameters of the parametric EQ filters to suppress offending frequencies upon detection were $p = 0.5012$ (-6 dB) and $q = 5$. The maximum number of parametric EQ filters were set to 12 in order to limit perceptual distortions in the output sound. Fig. 6(a)–6(c) shows signals with and without suppression against the desired signal. Clearly, the offending frequency suppression method quickly stopped the system from going into instability. Fig. 6(d) shows the adaptive notch filter tracking during the operation for the subband where an offending frequency occurred. It can be seen that, once howling started, the adaptive notch filter converged to the offending frequency and tracking became less variable. During instability both the energy monitoring counter and the ANF tracking counter grew as shown in Fig. 6(e). In Fig. 6(e), scaled-down values of the ANF tracking counter are shown for better presentation of both counters (γ_i^a and γ_i^r) on one axis. However, this does not affect the performance. In fact, the energy monitoring criterion was fulfilled before the ANF tracking criterion was met. However, the offending frequency was not detected until the ANF variance became smaller as indicated by the ANF tracking counters.

In the next experiment, we evaluate the offending frequency suppression scheme in terms of speed of detection and output sound quality. The output sound quality was judged with the PESQ measure from the steady state output sound. The speed of the offending frequency suppression method was calculated with the maximum time to recover from instability (mTRI) measure. The mTRI is an estimate of the duration of the longest

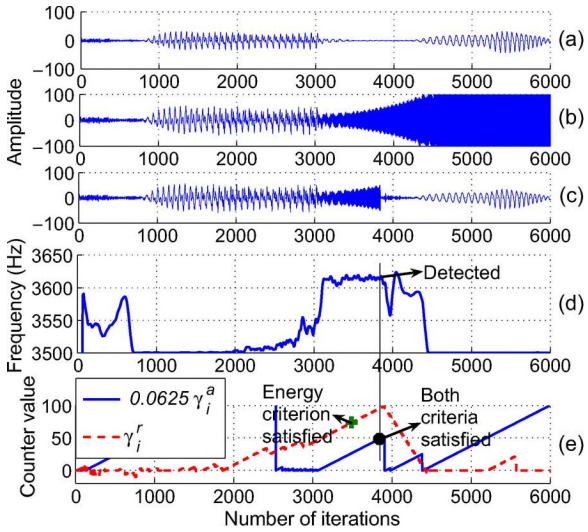

Fig. 6. (a) Desired amplified signal, (b) signal without suppression, (c) signal after OF detection and suppression, (d) ANF tracking, and (e) energy monitoring and ANF tracking counters in band 28 with center frequency of 3662.5 Hz.

TABLE VIII
MEASURES WITH AND WITHOUT RESET ALGORITHM

Measures	With reset			Without reset		
	Case 1	Case 2	Case 3	Case 1	Case 2	Case 3
N_h^s	1	3	3	3	5	8
N_h	19	30	48	18	30	44
mTRI (s)	0.2	0.2	0.4	0.1	0.2	0.4
PESQ	3.8	3.8	3.8	3.7	3.7	3.5

howling occurrence. Howling occurrences were manually identified according to the method described in [32]. Let the duration of the jth howling segment be Δt_j, then the mTRI is calculated as

$$\text{mTRI} = \max_{\forall j \in [1\ N_h]} (\Delta t_j) \tag{4}$$

where N_h is the number of offending frequencies detected. The parameters for the reset algorithm were $\lambda_l = 0.999$, $\lambda_h = 0.7$, $\epsilon_r = 10^{-12}$, $\delta_o = 0.1$, and $T_o = 10$. In this simulation, profile 4 and the six speech input signals of 80 seconds were used. Three acoustic feedback cases were studied. In the first case, feedback path 1 was used for the whole 80 seconds. Feedback path 2 was used for the whole experiment in the second case. In the third case, the experiment started with feedback path 1 and after 40 seconds, it was switched to feedback path 2. For the three feedback cases discussed above, total number of howling occurrences (N_h), mTRI and mean PESQ values were calculated and are listed in Table VIII. Table VIII also lists the average number of offending frequencies per experiment that remained for the different feedback cases in the steady state (N_h^s) with and without the use of the reset algorithm. Clearly, the number of steady state offending frequencies are typically smaller than the total number of howling occurrences (N_h) during the experiment for the reset algorithm because some of the offending frequencies gets reset.

The howling occurrences (N_h) in Table VIII indicate that ramping up gain to the target gain in the beginning and the feedback path change created several instances of howling. The number of howling occurrences were the most for the feedback case 3 because of the feedback path change. The effects of such occurrences were mitigated by the OFS method. The instability was detected in less that 0.5 s in all the experiments. The use of reset algorithm yielded in fewer number of parametric EQ filters in the steady state (N_h^s). However, this did not compromise the output sound quality as indicated by the PESQ values. On the contrary, use of the reset algorithm yielded slightly better output sound quality.

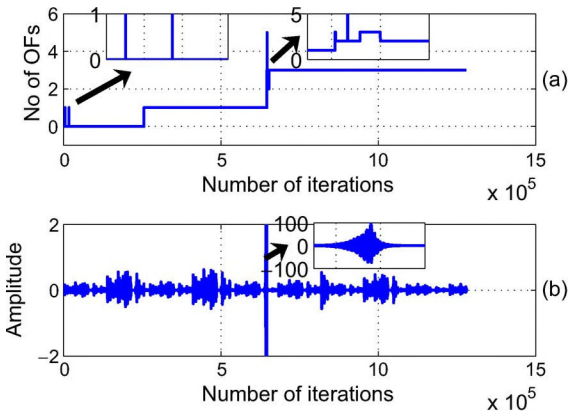

Fig. 7. (a) Number of offending frequencies and (b) the output signal with the OFS method.

The number of offending frequencies (OFs) and the output signal during the experiment for the feedback situation 3 and profile 4 are shown in Fig. 7(a) and 7(b), respectively. Fig. 7(a) also shows a zoomed in view of two half a second long intervals—one at the beginning of the experiment and the other when the feedback path changed to better understand the changes in the number offending frequencies. It can be seen that two offending frequencies were detected in the beginning when the hearing aid gain was ramping up to the desired value. These frequencies were reset later on. The third offending frequency that was detected later and was not reset during the course of the simulations as the adaptive filter was close to the steady state behavior at that time. When the feedback path changed, offending frequencies were detected, suppressed and reset several times. Finally, the output signal in Fig. 7(b) suggests that the offending frequency detection during the gain increase was quick enough to keep the system stable. However, the feedback path change sent the system into instability for a short period of time as shown in the 0.5-s long inset plot in Fig. 7(b).

In the next experiment, we explore maximum stable gains for various schemes—adaptive gain processing (AGP), offending frequency suppression (OFS), combined gain processing that includes adaptive gain processing with offending frequency suppression (AGP+OFS), and the fixed gain processing (FGP) method. The gain processing methods—AGP, OFS, and (AGP+OFS)—modified the forward path hearing aid gain along with the adaptive feedback cancellation. On the other hand, the hearing aid gain was fixed during the course of the experiment for the fixed gain processing method. The fixed gain processing method incorporated adaptive feedback cancellation for canceling the acoustic feedback. The feedback path 1 was used for this evaluation. The psychoacoustic measures, feedback and loudness ratings, for all the schemes at various flat hearing aid

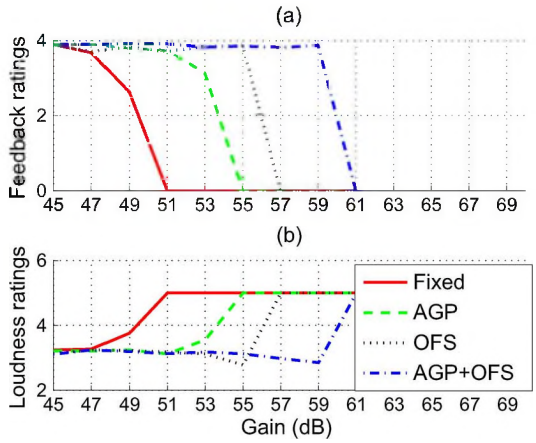

Fig. 8. (a) Feedback. (b) Loudness ratings for various methods.

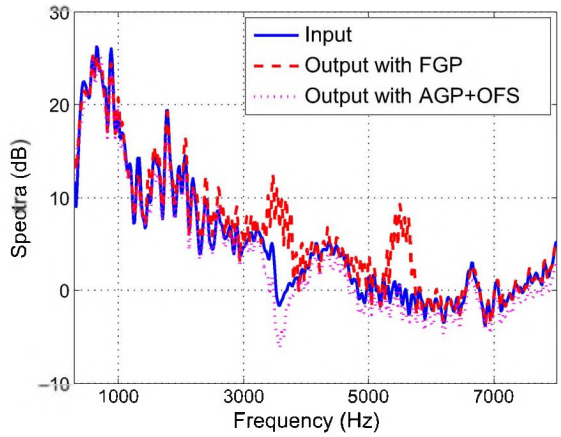

Fig. 9. Comparison of the output spectra of the two methods.

gain values are summarized in Fig. 8. In Fig. 8, the feedback rating (FR) of 0 or the loudness rating (LR) of 5 indicate that the system went into howling for that hearing aid gain. The subjective ratings of residual feedback and loudness for the input signal to the hearing aid were 4.1 and 3.1, respectively.

The following conclusions can be drawn from psychoacoustic measures in Fig. 8. The output sound quality deteriorated as indicated by the feedback ratings for fixed gain methods as the hearing aid gain was increased. The gain processing methods of this paper, individually and combined, maintained the output sound quality at higher hearing aid gains than the fixed gain method by suppressing unwanted acoustical feedback components. According to the feedback ratings in Fig. 8, it can be said that the fixed gain processing provided approximately 11 dB of maximum stable gain, the adaptive gain processing (AGP) provided 15 dB of maximum stable gain, the offending frequency suppression provided up to 19 dB of maximum stable gain and the combined gain processing (AGP+OFS) could provide 23 dB of maximum stable gain without deteriorating the sound quality due to the residual acoustic feedback. Furthermore, according to the loudness ratings in Fig. 8, the adaptive gain processing did not reduce loudness for all stable hearing aid gains, whereas the OFS and the combined gain processing (AGP+OFS) had slightly lower loudness ratings at higher gains before becoming unstable. The reduction in loudness in the OFS and AGP+OFS was due to use parametric EQ filters. Our studies indicate that the use of 6–8 parametric EQ filters did not affect loudness of the output sound. Comparing the ratings for the combined gain processing (AGP+OFS) at hearing aid gain values of 55–59 dB with the fixed gain processing at the hearing aid gain of 47 dB, it can be said that the combined gain processing presented in this paper provided 8 to 12 dB additional gain over traditional fixed gain processing with good output sound quality.

To better understand the gain processing methods of the paper, we compare the power spectra of the output produced with the fixed gain method and with the adaptive gain processing (AGP) method for a flat hearing aid gain of 49 dB as shown in Fig. 9. At this gain value, the fixed gain system was close to instability. The spectra were estimated using the Welch method by dividing data into frames of 512 samples with 256 sample overlap. There are noticeable differences between the spectra of the output of the fixed gain system and the input speech especially at frequencies near 3500 and 5500 Hz. These differences were due to residual feedback components that caused ringing/howling behavior in the output signal. The output of the combined gain processing scheme (AGP+OFS) did not exhibit residual feedback or howling effects. Specifically, the buildup near 5500-Hz frequencies was reduced just with the adaptive gain processing and with no use of parametric EQ filters. On the other hand, parametric EQ filters were used to reduce gain near 3500-Hz frequencies along with adaptive gain processing to eliminate the ringing/howling effects. Together, the combined gain processing (AGP+OFS) completely eliminated the residual feedback components as indicated by the feedback rating in Fig. 8. The gain processing resulted in slightly lower spectra than the input signal spectra especially at higher frequencies. However, these reductions did not reduce loudness according to loudness ratings in Fig. 8.

In the next experiment, the fixed gain system was evaluated against the adaptive gain processing (AGP), offending frequency suppression (OFS) and combined gain processing (AGP+OFS) on four hearing aid gain profiles using speech and music signals. Feedback path 2 was used for this experiment. The average subjective ratings for various profiles with all methods are summarized in Table IX. In Table IX, all methods provided good output sound quality for profiles 1 and 2 for both types (speech and music) of input signals. The fixed gain processing provided good output sound quality for profile 3 with speech signals, however, had soft whistling sounds in the output signal when music signals were input to the hearing aid system. On the other hand, all gain processing methods (AGP, OFS and AGP+OFS) yielded good output sound quality for both types of input signals with hearing aid gain profile 3. Finally, the fixed gain processing had significant residual feedback components in the output sound for the hearing aid profile 4 as indicated by the feedback ratings in Table IX. Use of the gain processing methods improved the output sound quality in every situation. Specifically, the gain processing methods suppressed the residual feedback components for it to be inaudible with every gain processing method except with the adaptive gain processing for music signals. The adaptive gain processing (AGP) produced output sound with intermittent residual feedback components in it when the input to the

TABLE IX
FEEDBACK AND LOUDNESS RATINGS

Profile	Signal	Measures	Fixed	AGP	OFS	AGP+OFS
1	SPEECH	Feedback rating	3.9	3.9	3.9	3.9
		Loudness rating	3.3	3.2	3.2	3.2
	MUSIC	Feedback rating	3.9	3.9	3.9	3.9
		Loudness rating	3.2	3.2	3.3	3.2
2	SPEECH	Feedback rating	3.9	3.9	3.9	3.9
		Loudness rating	3.2	3.3	3.2	3.2
	MUSIC	Feedback rating	3.9	3.9	3.9	3.9
		Loudness rating	3.2	3.2	3.2	3.2
3	SPEECH	Feedback rating	3.9	3.9	3.9	3.9
		Loudness rating	3.2	3.2	3.2	3.2
	MUSIC	Feedback rating	3.1	4.0	3.9	3.9
		Loudness rating	3.3	3.2	3.2	3.2
4	SPEECH	Feedback rating	2.2	3.9	3.7	4.0
		Loudness rating	3.9	3.2	3.3	3.2
	MUSIC	Feedback rating	0	2.9	3.8	3.9
		Loudness rating	5	3.4	3.2	3.2

hearing aid system was the music signal and gain profile 4 was used.

It is interesting to note that the traditional fixed gain system could not provide enough feedback cancellation in the case of profound hearing loss gain profile (profile 4) for an ITE hearing aid[5] used in the experiment. Often, audiologists suggest the use of behind-the-ear hearing aids for patients with profound hearing loss [29]. The results in Table IX indicate that the method of this paper will enable a patient with profound hearing loss to use an ITE hearing aid which is not possible otherwise. Consequently, the methods of this paper not only provide additional maximum stable gain but also enable patients to use more comfortable style hearing aids which is a big concern for many patients [29].

In the next experiment, the combined gain processing (AGP+OFS) was evaluated against the classical fixed gain processing method with a real-time feedback path. The experimental time setup used to obtain coefficients of the feedback paths, as described earlier in this section, was used for this experiment. The white board was placed parallel to the face plate of the ITE hearing aid at 100 cm in this experiment. The gain processing methods of this paper and the feedback cancellation algorithm with the fixed gain were implemented using an ADSP-21364 processor. With the above setup, output of the hearing aid system was recorded with a sound card for both schemes.

Residual feedback ratings and loudness ratings of the recorded data with both schemes were obtained with subjective evaluations. The average subjective ratings for both methods at different flat hearing gain values are summarized in Table X. As can be seen from the table, the ratings for the feedback and the loudness obtained from the test for combined gain processing at 18 dB above the critical gain (CG) is approximately same as those for the fixed gain at 10 dB above the CG. The output sound had significant residual acoustic feedback components for the fixed gain method at 12 dB above the CG. On the other hand, the good output sound quality was obtained with the combined gain processing (AGP+OFS) for gain values of 18 dB above the critical gain (CG). The output sound at 20 dB above the CG for the combined gain processing (AGP+OFS) exhibited intermittent ringing. The output sound quality was unacceptable due to substantial acoustic feedback components for the combined gain processing at 22 dB above the CG. The low perceptual ratings for the fixed gain processing at gain values 12 dB and higher along with the acceptable performance of the gain processing methods (AGP+OFS) for hearing aid gain values 18 dB and lower indicates the viability of the hearing aid system presented in this paper.

[5]The feedback path was derived from an ITE.

TABLE X
FEEDBACK (FR) AND LOUDNESS RATINGS (LR)

Gain above CG (dB)		8	10	12	14	16	18	20	22	24
Fixed gain processing	FR	4	4	2.2	0	0	0	0	0	0
	LR	3.2	3.1	3.6	5	5	5	5	5	5
AGP+OFS	FR	4	3.9	4.1	3.8	4	3.8	3.2	2.3	0
	LR	3.1	3.1	3	3.2	3.1	3.2	3.2	3.7	5

Finally, we evaluated effect of gain processing methods of this paper on speech intelligibility with a psychophysical experiment. In this experiment, 4 subjects were presented with sentences of 5 to 8 words at different signal-to-noise ratios and with the gain processing methods presented in this paper. The subjects were asked to repeat the sentence. All subjects had at least 4 years of college education. The experiment attempts to find the percent of correct words as a function of signal-to-noise ratio. A total 32 words were used to create the sentences. The sentences were recorded with a high-quality (Audio-Technica AT891R) microphone. Three American English speakers participated in the recording process. The speakers sat directly in front of the microphone during recordings. The distance between the microphone and the talkers was less than 2 feet for all the recordings. The RT60 of the room where the recordings took place was approximately 0.15 seconds. The signal-to-noise ratio of each of the recording was at least 50 dB.

These recordings were used in the adaptive feedback cancellation setup for the gain processing methods of this paper and the fixed gain processing method. The gain profiles 1 through 4 were used in the adaptive feedback cancellation. The outputs of the adaptive feedback cancellation was further corrupted with additive white noise to create different signal-to-noise ratios. Eleven signal-to-noise ratios ranging from -12 to 18 dB were used in the experiment. The effect of wide-band noise upon speech intelligibility is similar to that of low-pass filtered noises [33]. The processed signals in this way at different SNR values were presented to four American English-speaking subjects with normal-hearing through a pair of headphones. They were asked to listen to the sentences and reproduce them. The sentences were presented in a random order. Each word with a signal-to-noise ratio was presented at least 4 times to each subject.

The percentage (%) of correctly produced words as a function of the signal-to-noise ratio for various schemes and hearing loss profiles are shown in Fig. 10. The processed signals with the methods of this paper did not reduce intelligibility compared to the fixed gain processing for profiles 1 and 2. The output signals with the fixed gain processing for profiles 1 and 2 had good output sound quality as indicated by feedback and loudness ratings in Table IX. Comparable intelligibility for the processed

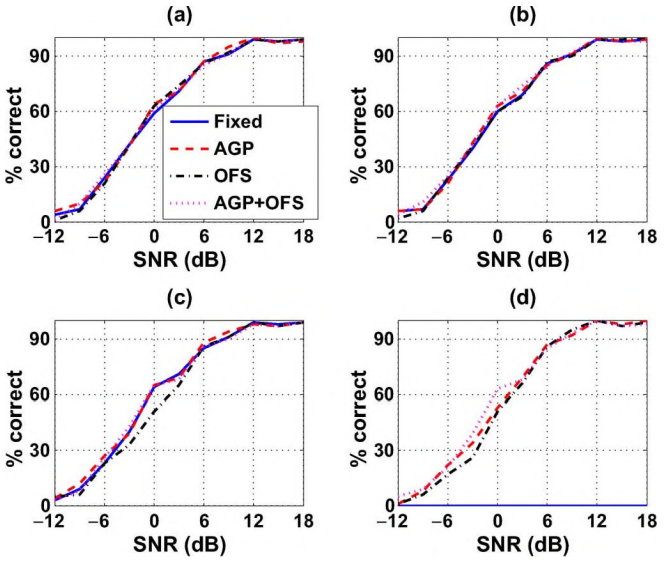

Fig. 10. Percentage of correct words with various schemes at different signal-to-noise ratios (SNRs).

signals with the methods of this paper for these profiles suggest that the gain processing presented in this paper did not compromise with the speech intelligibility. The speech intelligibility for profiles 3 and 4 was slightly lower for the offending-frequency suppression method at lower signal-to-noise ratios than the other methods. However, the speech intelligibility was comparable to the other methods at higher signal-to-noise ratios which is the more practical listening situations. We did not evaluate the fixed gain processing for profile 4 due to high residual acoustic feedback components in the output. The intelligibility is shown by 0 at all SNR values. The gain processing methods of this paper did not reduce intelligibility over traditional methods in situations where the latter provided good quality output signals. However, our method is able to provide acceptable speech intelligibility for a larger range of hearing impairments.

The gain processing methods of this paper improves the feedback cancellation efficiency by hearing aid gain processing in the forward path. Other nonstationary gain processing methods such as wide-dynamic-range-compression (WDRC) and noise reduction (NR) algorithms also change the hearing aid gain adaptively to improve the output sound quality. In our evaluations, we did not include these nonstationary gain processing methods to exclusively evaluate benefits of the gain processing methods presented in this paper. It is straightforward to combine the gain processing methods of this paper with the WDRC and NR. Specifically, the gain changes due to the WDRC and NR can be incorporated in the signal model that is used to calculate the masking thresholds. Moreover, the feedback detection algorithm can include the information of the gain processing due to WDRC in the calculations of energy growth if needed. Finally, the gain processing due to the noise reduction algorithms in hearing aids often reduce loudness [34], [35]. On the other hand, the gain processing presented in this paper is able to maintain the loudness as demonstrated by psychophysical experiments in this section.

V. Conclusion

This paper presented algorithms that modify the forward path gain in a hearing aid to improve adaptive feedback cancellation efficiency. The gain modification is based on perceptual redundancy in the input signal and gain reductions in narrowband frequency regions with parametric EQ filters. Psychophysical ratings from MATLAB simulations as well as experimental data with speech and music signals indicate that the gain modifications provide 8–12 dB of additional stable gain over traditional approaches. The reset algorithm successfully eliminated unnecessary filters placed in the signal path during the transient periods. Subjective assessment of the output of the hearing aid suggests that this paper's approach also delivers perceptually better output sound quality without compromising loudness in the output sound. Consequently, the hearing aid system presented in this paper may be a better alternative to currently used techniques for hearing aid signal processing.

References

[1] A. Kaelin, A. Lindgren, and S. Wyrsch, "A digital frequency domain implementation of a very high gain hearing aid with compensation for recruitment of loudness and acoustic echo cancellation," *Signal Process.*, vol. 64, pp. 71–85, 1998.

[2] J. A. Maxwell and P. M. Zurek, "Reducing acoustic feedback in hearing aids," *IEEE Trans. Speech Audio Process.*, vol. 3, no. 4, pp. 304–313, Jul. 1995.

[3] S. Wyrsch and A. Kaelin, "Subband signal processing for hearing aids," in *Proc. IEEE Int. Symp. Circuits Syst.*, Orlando, FL, Jul. 1999, vol. 3, no. 3, pp. 29–32.

[4] J. Hellgren, "Analysis of feedback cancellation in hearing aids with filtered-x lms and the direct method of closed loop indentification," *IEEE Trans. Speech Audio Process.*, vol. 10, no. 2, pp. 119–131, Feb. 2002.

[5] R. Wang and R. Harjani, "Suppression of acoustic oscillations in hearing aids using minimum phase techniques," in *Proc. IEEE Int. Symp. Syst. Circuits*, Minneapolis, MN, May 1993, pp. 3–6.

[6] M. R. Schroeder, B. S. Atal, and J. L. Hall, "Optimizing digital speech coders by exploiting masking properties of the human ear," *J. Acoust. Soc. Amer.*, vol. 66, pp. 1647–1652, Dec. 1979.

[7] J. M. Harte and S. J. Elliott, "A comparision of various nonlinear models of cochlear compression," *J. Acoust. Soc. Amer.*, vol. 117, no. 6, pp. 3777–3786, Jun. 2005.

[8] T. Painter and A. Spanias, "A review of algorithms for perceptual coding of digital audio signals," in *Proc. IEEE Int. Conf. Digitial Signal Process.*, Santorini, Greece, Jul. 1997, vol. 1, pp. 179–208.

[9] S. M. Kuo and J. Chen, "New adaptive IIR notch filter and its application to howling control in speakerphone system," *Electron. Lett.*, vol. 28, no. 8, pp. 764–766, Apr. 1992.

[10] V. Hamacher, J. Chalupper, J. Eggers, E. Fischer, U. Kornagel, H. Puder, and U. Rass, "Signal processing in high-end hearing aids: State of the art, challenges, and future trends," *EURASIP J. Appl. Signal Process.*, vol. 18, pp. 2915–2929, 2005.

[11] D. Troxel, "Method and Apparatus for Identifying Feedback in a Circuit," U.S. patent 20060215852A1, Sep. 28, 2006.

[12] A. Pandey, V. J. Mathews, and M. Nilsson, "Adaptive gain processing to improve feedback cancellation in digital hearing aids," in *Proc. IEEE Int. Conf. Acoust., Speech, Signal Process.*, Las Vegas, NV, Apr. 2008, pp. 357–360.

[13] A. Pandey and V. J. Mathews, "Improving adaptive feedback cancellation in digital hearing aids through offending frequency suppression," in *Proc. IEEE Int. Conf. Acoust., Speech, Signal Process.*, Dallas, TX, Mar. 2010, pp. 173–176.

[14] M. Harteneck, S. Weiss, and R. W. Stewart, "Design of near perfect reconstruction oversampled filter banks for subband adaptive filters," *IEEE Trans. Circuits Syst.*, vol. 46, no. 8, pp. 1081–1086, Aug. 1999.

[15] S. Weiss, A. Stenger, R. W. Stewart, and R. Rabenstein, "Steady-state performance limitations of subband adaptive filters," *IEEE Trans. Signal Process.*, vol. 49, no. 9, pp. 1982–1991, Sep. 2001.

[16] M. Rosch and B. Imfeld, "Subband Adaptive feedback cancellation for hearing aids on an OrelaTM 4500 DSP," M.S. thesis, Hochschule Fur Technik Rapperswil, Rapperswil, Switzerland, 2005.

[17] L. Theverapperuma. "Adaptive feedback cancellation for hearing aids: Theories. algorithms. computations. and systems." Ph.D. dissertation. University of Minnesota. Minneapolis. 2007.
[18] R. Brennan and T. Schneider. "A flexible filterbank structure for extensive signal manipulations in digital hearing aids." in *Proc. IEEE Int. Symp. Circuits Syst.*. Monterey. CA. Jun. 1998. vol. 6. no. 31. pp. 569–572.
[19] R. E. Crochiere and L. R. Rabiner. *Multirate Digital Signal Processing*. Upper Saddle River. NJ: Prentice-Hall. 1996.
[20] R. Dong. D. Hermann. R. Brennan. and E. Chau. "Joint filterbank structures for integrating audio coding into hearing aid applications." in *Proc. IEEE Int. Conf. Acoust., Speech. Signal Process.*. Las Vegas. NV. Apr. 2007. pp. 1533–1536.
[21] B. Farhang-Boroujeny. *Adaptive Filter: Theory and Applications*. Chichester. U.K.: Wiley. 1998.
[22] E. Zwicker and H. Fastl. *Psychoacoustics: Facts and Models*. 2nd ed. Berlin. Germany: Springer Verlag. 1999.
[23] J. M. Kates. "Feedback cancellation in hearing aids: Results from a computer simulation." *IEEE Trans. Signal Process.*. vol. 39. no. 3. pp. 553–562. Mar. 1991.
[24] P. A. Regalia and S. K. Mitra. "Tunable digital frequency response equalization filters." *IEEE Trans. Acoust., Speech. Signal Process.*. vol. 35. no. 1. pp. 118–120. Jan. 1987.
[25] R. Martin. "An efficient algorithm to estimate the instantaneous SNR of speech signals." in *Proc. Eurospeech*. Berlin. Germany. Sep. 1993. vol. 3. pp. 1093–1096.
[26] J. Hellgren. "Variations in the feedback of hearing aids." *J. Acoust. Soc. Amer.*. vol. 106. no. 5. pp. 2821–2833. Nov. 1999.
[27] S. H. Lotterman. R. N. Kasten. and D. M. Majerus. "Battery life and nonlinear distortion in hearing aids." *J. Speech Hear. Disorders*. vol. 32. pp. 274–278. Aug. 1967.
[28] J. M. Kates. "Cross-correlation procedures for measuring noise and distortion in agc hearing aids." *J. Acoust. Soc. Amer.*. vol. 107. no. 6. pp. 3407–3414. 2000.
[29] H. Dillon. *Hearing Aids*. 1st ed. New York: Thieme. 2001.
[30] D. Byrne and W. Tonisson. "Selecting the gain of hearing aids for persons with sensori-neural hearing impairments." *Scand. Audiol.*. vol. 5. no. 1. pp. 51–59. 1976.
[31] "Perceptual evaluation of speech quality (PESQ): An objective method for end-to-end speech quality assessment of narrow band telephone networks and speech coders." ITU-T Rec. P.862. Feb. 2001.
[32] T. van Waterschoot and M. Moonen. "Adaptive feedback cancellation for audio applications." *Signal Process.*. vol. 89. no. 11. pp. 2185–2201. Nov. 2009.
[33] G. A. Miller and P. A. Nicely. "An analysis of perceptual confusions among some english consonants." *J. Acoust. Soc. Amer.*. vol. 27. pp. 338–352. 1955.
[34] N. I. Whitmal and A. Vosoughi. "Recruitment-of-loudness effects of attenuative noise reduction algorithms." *J. Acoust. Soc. Amer.*. vol. 111. no. 5. pp. 2380–2380. 2002.
[35] S. Krishnamurti and L. Anderson. "Digital noise reduction processing in hearing aids: How much and where?," *Hear. Rev.*. Mar. 2008.

Ashutosh Pandey received the B.S. degree in electronics and communications engineering from the Institute of Technology-Banaras Hindu University (IT-BHU). Varanasi. India. and the Ph.D. degree in electrical and computer engineering from the University of Utah. Salt Lake City.

Currently. he is a Senior DSP Research Engineer for ClearOne Communications. Salt Lake City. His research interests are in applications of signal processing algorithms for audio conferencing products and hearing aids.

V. John Mathews (S'82–M'84–SM'90–F'02) received the B.E. (Honors) degree in electronics and communication engineering from the University of Madras. Chennai. India. in 1980 and the M.S. and Ph.D. degrees in electrical and computer engineering from the University of Iowa. Iowa City. in 1984 and 1981. respectively.

He is a Professor of Electrical and Computer Engineering at the University of Utah. Salt Lake City. At the University of Iowa. he was a Teaching/Research Fellow from 1980 to 1984 and a Visiting Assistant Professor in the Department of Electrical and Computer Engineering during the 1984–1985 academic year. He joined the University of Utah in 1985. where he is engaged in teaching signal processing classes and conducting research in signal processing algorithms. He served as the Chairman of the Electrical and Computer Engineering Department from 1999 to 2003. His current research interests are in nonlinear and adaptive signal processing and application of signal processing techniques in audio and communication systems. biomedical engineering. and structural health management. He has also contributed in the areas of perceptually tuned image compression and spectrum estimation techniques. He is the author of the book *Polynomial Signal Processing* (Wiley. 2000) and coauthored with Prof. G. L. Sicuranza. University of Trieste. Italy. He has published more than 125 technical papers.

Dr. Mathews has served as a member of the Signal Processing Theory and Methods Technical Committee. the Education Committee and the Conference Board of the IEEE Signal Processing Society. He was the Vice President (Finance) of the IEEE Signal Processing Society during 2003–2005. and is now serving a three-year term as the Vice President (Conferences) of the Society. He is a past associate editor of the IEEE TRANSACTIONS ON SIGNAL PROCESSING and the IEEE SIGNAL PROCESSING LETTERS. and has served on the editorial board of the IEEE SIGNAL PROCESSING MAGAZINE. He currently serves on the editorial board of the IEEE JOURNAL OF SELECTED TOPICS IN SIGNAL PROCESSING. He has served on the organization committees of several international technical conferences including as General Chairman of IEEE International Conference on Acoustics. Speech. and Signal Processing (ICASSP) 2001. He is a recipient of the 2008–2009 Distinguished Alumni Award from the National Institute of Technology. Tiruchirappalli. India.